RSC Advances

PAPER

View Article Online
View Journal | View Issue

Cite this: *RSC Adv.*, 2022, **12**, 6811

Crosslinking of dialdehyde heparin: a new strategy for improving the anticoagulant properties of porcine acellular dermal matrix

Rongxin Feng, [a] Nianhua Dan, *[ab] Yining Chen [ab] and Weihua Dan[ab]

The anticoagulant properties of valve materials are essential to maintain blood patency after artificial valve implantation. Porcine acellular dermal matrix (pADM) has low immunogenicity, good biocompatibility, and can reduce calcification by eliminating heterogeneous cells. However, its main component is collagen, which has strong coagulation function and poor anticoagulant activity. When used in heart valve materials, it can easily coagulate and form a life-threatening thrombus. Therefore, it is necessary to improve its anticoagulant performance. The glutaraldehyde (GA) cross-linked valves widely used clinically are easy to calcify with poor anticoagulant performance and cytotoxicity. In this study, dialdehyde heparin containing cross-linking active aldehyde groups was prepared by sodium periodate oxidation, then it was used for crosslinking with pADM to chemically modify its anticoagulant performance. Compared with GA cross-linked pADM (GA-pA), dialdehyde heparin cross-linked pADM (OL-pA) has better thermal stability and biocompatibility, especially its anticoagulant and antiplatelet adhesion were significantly improved, which can reduce the incidence of coagulation, thrombocytopenia and bleeding. In summary, dialdehyde heparin is expected to be applied to modify the anticoagulant properties of pADM and has great potential for the preparation and clinical application of anticoagulant materials such as heart valves and artificial blood vessels.

Received 11th December 2021
Accepted 22nd February 2022

DOI: 10.1039/d1ra08982j

rsc.li/rsc-advances

Introduction

Heart valve diseases such as congenital defects, rheumatic fever, infectious endocarditis and valve calcification are common heart diseases. Heart valve lesions in humans can lead to valve stenosis, reflux and heart failure, which seriously affect the health of patients.[1,2] As an effective treatment of cardiac valvular disease, artificial heart valve replacement surgery is widely used in clinical practice. The commonly used artificial valve replacement materials are biological valve and mechanical valve. Biological valve has good histocompatibility and anti-thrombosis, but it is easily subject to calcification, and the durability after implantation is short. Mechanical valve has good durability, but it is easily complicated with thrombosis and needs long-term anticoagulant therapy.[3,4] The poor anticoagulant performance of artificial heart valves will lead to coagulation, and the resulting valve thrombosis, vascular embolism and bleeding are common high-risk complications in artificial heart valve replacement surgery.[5] Platelets and fibrin in the blood will adhere to the valve tissue to form a nonbacterial thrombotic endocarditis (NBTE) after coagulation and clots, which is the bacterial transmission site of infectious endocarditis.[6] It will increase the contact time and contact area between cells and bacteria, and accelerate the growth and reproduction of bacteria, which will greatly increase the incidence of complications such as blood embolism, valve damage, and infection of endocarditis in patients after operation.[7] After cardiac valve replacement surgery in China and abroad, in order to prevent coagulation, thrombosis and endocarditis infection, the patients need to adhere to taking anticoagulant drugs every day to maintain a normal life. Insufficient or excessive medication will lead to postoperative complications and even death, which seriously reduces the success rate of artificial heart valve replacement surgery and affects the quality of life and recovery of patients. Therefore, it is of great significance to develop a new generation of artificial heart valves with excellent anticoagulant performance.

In recent years, many researchers have attempted to construct new heart valves through tissue engineering technology, hoping to improve the anticoagulant performance of valve materials and prolong the service life of artificial valves. The acellular heart valve is a kind of very important tissue engineering heart valve (TEHV) scaffold material. Acellular tissue can retain the structure and performance of natural heart valves, has excellent biocompatibility and biodegradability, which can promote cell migration and differentiation. At present, it has been widely used as a valve replacement in the clinical implantation treatment of heart valve

[a]*Key Laboratory of Leather Chemistry and Engineering of the Education Ministry, Sichuan University, Chengdu, Sichuan 610065, China. E-mail: 201054776@qq.com; dannianhua@scu.edu.cn*

[b]*Research Center of Biomedical Engineering, Sichuan University, Chengdu, Sichuan 610065, China*

diseases.[8,9] Porcine acellular dermal matrix (pADM) is extracted all cellular components of the entire epidermis and dermis from pig skin, thereby retaining collagen fibers and basic tissue structures. Compared with other acellular tissue materials, pADM has multiple advantages for use in tissue-engineered heart valve scaffolds because of its low immunogenicity and good biocompatibility, and reduce calcification by removing heterogeneous cells, can also provide natural adhesion sites for cells, promote cell adhesion.[10,11] The main component of pADM is collagen, the coagulation activity of pure collagen is strong, its use as an implant material will activate platelets to release coagulation factors and accelerate blood coagulation to form thrombosis, which will seriously affect the patency of blood in the body after heart valve implantation. It is extremely easy to cause surgical complications such as vascular embolism, thrombocytopenia and bleeding, and even threaten patients' lives.[12] In addition, pure collagen has low thermal stability, poor mechanical strength and enzyme resistance,[13,14] it cannot meet the long-term implantation requirements of tissue-engineered heart valve scaffolds. In order to solve these problems, chemical crosslinking modification has been widely used to improve the physicochemical properties of pADM. Glutaraldehyde (GA) is usually used for cross-linking modification in clinics at present, but the anticoagulant and biocompatibility of GA cross-linked materials are poor, it will cause adhesion of platelets and fibrin as well as infiltration of blood cells and plasma components after implantation, and are highly susceptible to thrombosis, obstruction and calcification.[15] Thus, other cross-linking agents need to be selected to effectively improve the anticoagulation, antiplatelet adhesion and blood safety of pADM while taking into account the biocompatibility of materials.

Low molecular weight heparin (LMWH) is a polysaccharide mixture of repeating disaccharide units consisting of glyoxylate and glucosamine linked by 1,4-bonds. It has obvious anticoagulant and antithrombotic properties,[16,17] good biocompatibilities, low bleeding risk, and promotes cell proliferation.[18,19] It is an important anticoagulant commonly used in the clinic, has been widely used for surface anticoagulant property modification of cardiovascular materials.[20] The chemical modification of pADM with LMWH can balance the negative effect of collagen on blood coagulation and improve the anticoagulant activity of pADM. While the binding mode of LMWH to pADM is physical adsorption, only a small amount of LMWH molecules can be complexed with collagen in pADM by ionization. The density of LMWH grafted on the surface of pADM is low, the anticoagulant activity is uncontrollable. The introduction of LMWH molecules into decellularized heart valves through the covalent bond is expected to overcome these shortcomings. In this study, oxidized low molecular heparin (OL) containing cross-linked active aldehyde groups was produced by oxidation of sodium periodate, pADM was cross-linked and modified with different dosages of OL. OL was introduced into pADM material as an anticoagulant activity factor, and the anticoagulant performance, antiplatelet adhesion, enzymatic degradation resistance and biocompatibility of the cross-linked material were further tested and evaluated *in vitro* and *in vivo* (Fig. 1). We expect to develop a tissue engineering heart valve with excellent anticoagulant performance, enzymatic degradation resistance and biocompatibility.

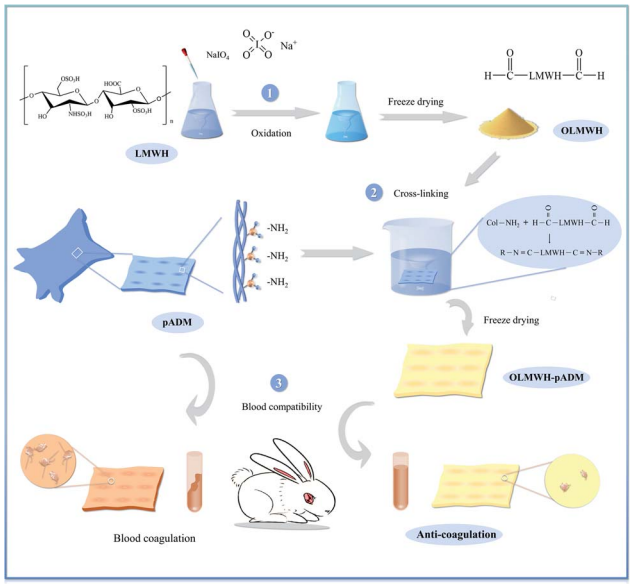

Fig. 1 Schematic illustration of preparing oxidized low molecular heparin (OL), and modification of anticoagulant properties of pADM by OL crosslinking agent based on Schiff base reaction.

Experiments and methods

Materials

pADM was provided by Jiangyin Benxiang Biotechnology Co., Ltd. (Jiangsu, China). Low molecular weight heparin (LMWH) was purchased from Baichuan Biotechnology Co., Ltd. (Xi'an, China). Mouse fibroblasts. Unless otherwise specified, all other chemicals and reagents were purchased from Kelong Chemical Reagent Co., Ltd. (Chengdu, China). All solvents used are analytical grade.

Preparation of oxidized low molecular heparin (OL)

3.66 g LMWH (150 U mg^{-1}, $M_r \approx 5000$ Da) was dissolved in 50 mL distilled water and continuously stirred at 37 °C for 2 h to obtain a uniform solution. Then 200 mL 0.25 M sodium periodate solution was added. The mixture was fully mixed and placed in the dark at 4 °C for 48 h. After the reaction, an excess of ethylene glycol was added to terminate the reaction. The sample was dialyzed in pure water at 4 °C for 3 days, change water 6 times a day. After that, the sample was freeze dried and weighed, named the resulting oxidation product as OL.

pADM treatment with OL

The pADM was cut into small pieces, and treated with different dosage of OL. About 0 g, 0.4 g, 0.8 g, 1.2 g, 1.6 g of OL and 1.2 g of LMWH were weighed and dissolved by adding 50 mL sodium carbonate buffer solution (pH 9.4). After that, 10 g of pADM was added to the above solutions, the resulting mixture was magnetically stirred at 37 °C for 48 h. After the reaction completion, the solution of 0.1 M NH_4Cl was added to terminate the reaction.

Each sample was thoroughly washed and freeze-dried, then denoted the samples separately as pADM, 4%-OL-pA, 8%-OL-pA, 12%-OL-pA, 16%-OL-pA, 12%-LH-pA. PADM crosslinked with 0.5% glutaraldehyde (GA) solution, denoted as GA-pA, was used as the control. The seven sample groups were stored in a controlled dry container at room temperature before testing.

Determination of oxidation degree of OL

The aldehyde content of OL was determined by hydroxylamine hydrochloride potentiometric titration, and then the oxidation degree was calculated.[21]

UV spectral measurements

The LMWH and OL samples were prepared into 1 mg mL^{-1} homogeneous solution, and the UV-Vis spectrophotometer was used to determine the UV absorption spectra of the samples in the wavelength range of 190–400 nm with distilled water as the reference.

FTIR spectral measurements

LMWH, OL, OL-pA, LH-pA and pADM samples were respectively mixed and pressed with potassium bromide at a ratio of approximately 1 : 100 (mg^{-1}), then placed in a FTIR spectrophotometer (SpectrumOne, PerkinElmer, Inc., Waltham, MA) for detection. The scanning wave number was set to 500–4000 cm^{-1}, the resolution was 4 cm^{-1}, and the scanning times were 32 times. Room temperature 25 °C, relative humidity < 65%.

Scanning electron microscopy

Scanning electron microscope (SEM; Hitachi S3000N, Hitachi, Ltd., Japan) was used to observe the morphology of OL-pA, LH-pA and pADM samples. All samples were sputter coated with gold and imaged at an accelerating voltage of 5 kV.

DSC measurements

Differential scanning calorimetry (DSC) analysis was conducted at a temperature range from 20 to 150 °C under a nitrogen atmosphere. Samples of 3–5 mg of OL-pA, LH-pA and pADM were loaded in the DSC aluminum pan, whereas an empty aluminum pan was used as reference. The heat ingrate was maintained at 5 K min^{-1}, and the N_2 flow was kept at 60 mL min^{-1}.

Thermogravimetric analysis

Thermogravimetric (TG) analysis was performed on a thermal analyzer (Netzsch TG 209, Germany). All measurements were conducted under a nitrogen atmosphere. A 3–5 mg of OL-pA, LH-pA and pADM were pressed into a cylindrical holder and heated from 50 to 800 °C at a heating rate of 20 K min^{-1}.

Hydrophobicity–hydrophilicity test

The moisture rate, the water absorption rate and the capillary water absorption rate of the specimens were measured. The samples were cut into squares with a side of 50 mm and placed in an environment with room temperature and humidity of about 65% for 24 h. Then, the dry samples were weighed (W_0), and soaked in distilled water for 24 h. After that, the samples were pressed with clean tweezers and hung in the air for 30 seconds and weighed (W_1). The filter paper was used to dry the moisture on the surface of the material and samples were again weighed (W_2). Finally, the samples were weighed (W_3) after centrifuging at a speed of 10 000 rpm for 15 min. The moisture rate, the water absorption rate and the capillary water absorption rate were calculated by the following equations, each test was conducted on five samples and the average was calculated.

$$\text{Moisture rate (\%)} = (W_1 - W_0)/W_0 \times 100\% \quad (1)$$

$$\text{Water absorption rate (\%)} = (W_2 - W_0)/W_0 \times 100\% \quad (2)$$

$$\text{Capillary water absorption rate (\%)} = (W_3 - W_0)/W_0 \times 100\% \quad (3)$$

Degradation properties

Bacterial type I collagenase was used to detect the enzymatic degradation resistance of the samples.[22] The samples of OL-pA, LH-pA and pADM (weighed as W_1) were incubated with bacterial type I collagenase (1 U mL^{-1}, 3 mL mg^{-1} of sample) at 37 °C. At each time point (1 d, 2 d, 4 d, 7 d), the samples were removed from the medium and were weighed (W_2) after washing with distilled water and lyophilizing. The proportion of degradations were calculated by the following equations, each test was conducted on five samples and the average was calculated.

$$\text{Proportion of degradation (\%)} = (W_1 - W_2)/W_1 \times 100\% \quad (4)$$

Cytocompatibility studies

The fibroblasts (L929) cultured to the logarithmic phase were used as model cells, and the cytocompatibility of OL-pA, LH-pA and pADM were evaluated by the CCK-8 method. Before cell inoculation, the samples were sterilized in an autoclave at 120 °C for 30 min. Then, it was transferred to the sample in a 96-well plate to dispense a cell suspension (200 μL) with a density of 5×10^4 cells per mL. After 24 h, the samples were transferred to another 96-well plate, and 200 μL of fresh medium and 20 μL of Cell Counting Kit-8 (CCK-8, Dojindo Laboratories, Kumamoto, Japan) solution were added, and then incubated at 37 °C for 3 h. Finally, 100 μL of the medium was distributed to another 96-well plate, and a spectrophotometer was used to measure the formazan dye colorimetrically, and the OD reading was recorded.

Hemolysis rate test

The sterile samples were placed in the test tube, and 10 mL of normal saline and 0.2 mL of fresh anticoagulant rabbit blood were added to each tube and fully mixed. 10 mL of distilled water and 0.2 mL of fresh anticoagulant rabbit blood were added to the test tube as positive controls, and 10 mL of normal saline and 0.2 mL of fresh anticoagulant rabbit blood were added as negative controls. The samples were cultured at 37 °C for 1 h, then centrifuged at 10 000 rpm for 10 min. The

hemolysis rate was calculated by the following equation, each sample was measured three times in parallel.

Platelet adhesion test

The sterile samples were placed in 24-well plates and the fresh anticoagulant rabbit blood was centrifuged at 10 000 rpm for 15 min to obtain platelet-rich plasma (PRP). 200 μL of PRP was completely coated on the surface of the sample and incubated at 37 °C for 2 h. The sample was rinsed twice with normal saline, and a certain amount of 2.5% glutaraldehyde solution was taken to fix the sample for 3 h. Then, 50%, 70%, 90% and 100% ethanol solutions were successively used for gradient dehydration. The samples were dried and sprayed with gold, and the platelets adhered to the material surface were observed by scanning electron microscopy.

In vitro anticoagulant activity test

The samples were dissolved in normal saline to prepare a 0.5 mg mL^{-1} solution. The pADM sample was used as the negative control, and the GA-pA was used as the positive control. The activated partial thromboplastin time (APTT), prothrombin time (PT) and thrombin time (TT) of the semi-automatic coagulation analyzer were measured with fresh rabbit plasma.

Statistical analysis

Each experiment had at least three replicates, all data were expressed as mean ± standard deviation. One-way ANOVA was used to measure differences in multiple datasets, and an intra-group *T*-test was used to measure data differences between groups with significant differences. The value of $P < 0.05$ is considered to have statistical significance, represented by *.

Results and discussion

Structural characterization of OL

The activity of polysaccharides is directly related to their molecular structure. UV and FTIR spectrum are commonly used to detect the purity of samples and analysis functional groups. Fig. 2a shows the UV spectra of LMWH and OL, it can be seen that both LMWH and OL have a sharp characteristic absorption peak between 190 and 220 nm, which is due to the electronic transition of the carboxylate chromophore of the glucuronic acid in the molecular chain. Other than that, no other peak shape changes were detected, indicating that the main molecular structure of both did not change significantly, and OL still retained the natural molecular structure of LMWH.

Fig. 2b shows the FTIR spectrum of LMWH and OL, it was found that both of them had characteristic absorption peaks at 892 cm^{-1} and 936 cm^{-1}.[23,24] The C–O–S stretching vibration absorption peak of the sulfuric acid group on amino hexose appeared around 830 cm^{-1}, the strong absorption peak of O–S stretching vibration appeared around 1240 cm^{-1}, and the C=O stretching vibration peak of the sulfuric acid group in the carboxyl group appeared around 1621 cm^{-1} was also found in both, all of these indicated that the main structure of the OL

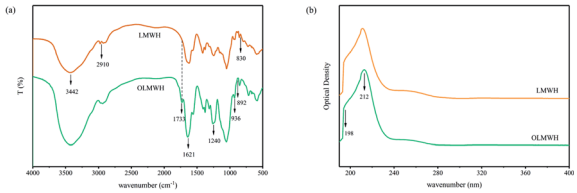

Fig. 2 (a) UV spectra of LMWH and OL, (b) FTIR spectra of LMWH and OL.

obtained after oxidation did not change significantly. It has been known that the reason for the conspicuous anticoagulant activity and cytocompatibility of LMWH is the presence of a reactive pentose structure in its molecular chain,[25] they can bind to antithrombin III (AT III), change the conformation of the antithrombin molecules, and inhibit the activity of coagulation factors IIa, Xa and IXa, exhibiting strong anticoagulant properties. The similarity of molecular structure between OL and LMWH is of great significance to retain the anticoagulant activity of OL. Different from LMWH, the OL obtained after oxidation showed the C=O stretching vibration peak of the aldehyde group at 1733 cm^{-1} wavenumber,[26] the C–H stretching vibration peak on the saturated carbon at 2910 cm^{-1} was weakened, and the hydroxyl absorption peak at 3442 cm^{-1} was slightly weakened, moving slightly to a low wavenumber. The oxidation degree of OL was determined by hydroxylamine hydrochloride potentiometric titration and calculated to be 45.41%, indicating that the hydroxyl group in LMWH molecular chain was successfully oxidized to aldehyde group by sodium periodate. The above results indicated that the oxidation of LMWH by sodium periodate can successfully introduce chemically active aldehyde groups based on retaining the natural molecular structure of LMWH, creating conditions for its application in the cross-linking modification of pADM.

Structural characterization of OL-pA

The main component of pADM is type I collagen, the characteristic absorption bands, typical absorption peaks and the secondary spatial structure of collagen can be characterized by FTIR (Fig. 3). It has already been reported,[27,28] that the amide I band located in approximately 1650 cm^{-1} is mainly caused by the C=O stretching vibration of the collagen molecule., the amide II band at 1540 cm^{-1} is caused by the bending vibration of N–H and the stretching vibration of C–N in the collagen molecule. The secondary spatial structure of collagen mainly includes α-helix, β-sheet, β-angle and random curly stacks. It is known that the amide I and amide II bands of collagen were directly related to the secondary structure of collagen.[29] The amide III band at 1235 cm^{-1} is generated by the in-plane bending vibration of C–N stretching and N–H in the amide bond, as well as the synergistic absorption peaks of the main chain $-CH_2$ group and the side chain glycine and proline swing vibrations. The amide A and amide B bands at 3440 cm^{-1} and 3080 cm^{-1} are due to the stretching vibration of the N–H groups. It can be observed that the characteristic absorption bands, typical absorption peaks and the secondary spatial

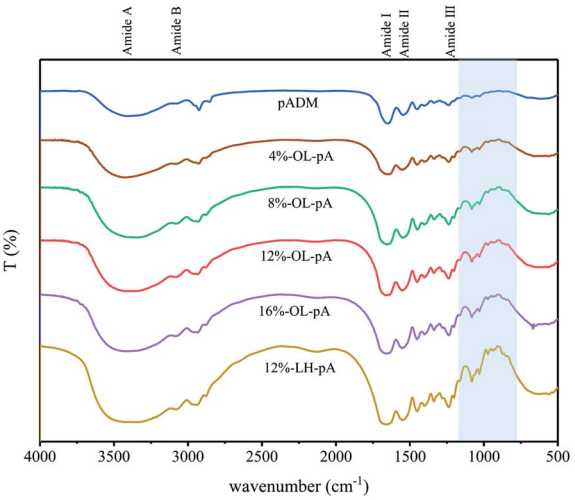

Fig. 3 FTIR spectra of pADM, LH-pA and OL-pA crosslinked with different dosage of OL.

structure of OL-pA had not changed after crosslinking with different doses of OL, indicating that pADM still retains the natural structure of collagen after crosslinking with OL. Compared with pADM, the characteristic peaks of LMWH appeared at 936 cm^{-1} and 892 cm^{-1} in OL-pA crosslinking with LMWH. The absorption peak of glycosidic bond appeared at 1080 cm^{-1}, and the peak shape was significantly enhanced and sharpened with the increase of OL dosage, which indicated that the OL structural unit was attached to the pADM, and the increase of OL dosage would introduce more heparin molecules into the collagen, thus increasing the degree of cross-linking degree of pADM. Meanwhile, the peak shape of the amide A band broadened after the introduction of OL and slightly shifted toward the lower wavenumber. The peak intensity of the amide I band slightly weakened, indicating that the aldehyde group in the OL molecular chain reacted with the $-NH_2$ of collagen to form a large number of stable Schiff base bonds. Therefore, it was tentatively inferred that OL and pADM were chemically crosslinked and grafted onto the surface of pADM without affecting the natural structure of collagen.

The surface morphology of the material has a direct impact on the growth and reproduction of cells.[30] Scanning electron microscopy (SEM) was used to observe the microstructure of crosslinked materials. As shown in Fig. 4, the collagen fiber bundles in pADM were interlaced and interwoven, there are irregular pores between fibers, and these pores were found to facilitate cell growth and adhesion.[31] Compared with the pADM, the fiber bundles in the OL-pA and LH-pA groups were thicker and stronger, the natural basic 3D structure of collagen fibers remained unchanged, and the porosity remained high. The 8%-OL-pA and 12%-OL-pA fibers are closely connected, and the fiber orientation is orderly without fiber breakage. The pores on the surface of the material can provide a suitable growth environment for cells and induce cell adhesion and proliferation on the surface of the material. The above results showed that OL has a good cross-linking effect on pADM, the microstructure of

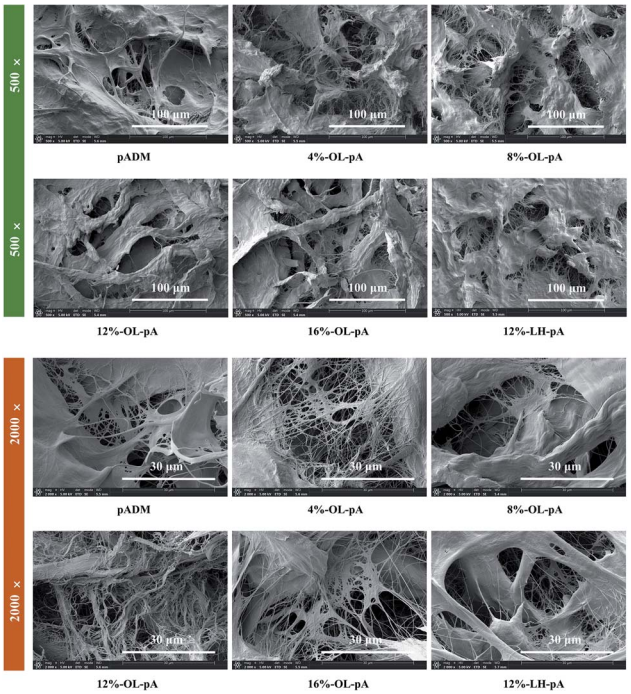

Fig. 4 SEM micrographs of pADM, LH-pA and OL-pA crosslinked with different dosage of OL (500×, 2000×).

the crosslinked material has no significant changes except for slight changes in pore size, and the porosity of the material surface is high, which is conducive to cell adhesion and growth.

Thermal stability analysis

The good stability of the artificial heart valve is the key to maintaining the normal physiological function of the valve can be maintained after being implanted into the human body. Differential scanning calorimetry (DSC) was used to evaluate the thermal stability of crosslinked collagen. Fig. 5a shows different endothermic peaks of pADM, LH-pA and OL-pA crosslinked with different dosage of OL. The DSC curves of all samples showed similar trends in the temperature range from 20 to 150 °C. The T_g of pADM was about 65.9 °C, and the T_g of LH-pA was about 72.8 °C, which was not much different from that of pADM, while the T_g of each group of OL-pA was significantly elevated. The T_g of OL-pA increased with the increase of OL dosage, and it reached the maximum value of about 87.3 °C when the OL dosage was 12%, with the dosage of OL increase to 16%, the T_g did not change much. This is because the aldehyde group in OL can combine with the reactive amino group in pADM to form Schiff base, which belongs to covalent bond and has stronger binding effect. The generation of new crosslinking bonds can effectively improve the thermal denaturation temperature of the material. While LMWH binds to pADM by physical adsorption, only a small amount of heparin molecules can ionize with collagen in pADM. Compared with the strong chemical interaction between OL and pADM, the introduction of LMWH did not produce a large increase in the thermal denaturation temperature of pADM. In conclusion, the study found that the T_g of OL-pA increased after crosslinking

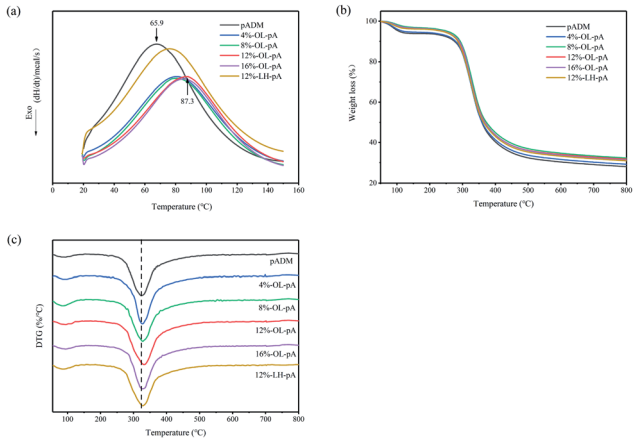

Fig. 5 (a) DSC patterns, (b) TG and (c) DTG analysis of pADM, LH-pA and OL-pA crosslinked with different dosage of OL.

modification, indicating that the cross-linked collagen structure was more stable and had higher thermal stability.

Thermogravimetric analysis (TGA) was used to further detect the structural stability of materials. Fig. 5b and c show the TG and DTG curves of pADM, LH-pA and OL-pA. It can be seen that the thermal decomposition of all samples is divided into two stages. The first stage of weight loss in the temperature range of 50 to 150 °C is mainly due to the evaporation of free water and the breakage of hydrogen bonds within the collagen molecules.[32] The second stage of weight loss in the temperature range of 200 to 800 °C is mainly due to the thermal decomposition of the samples, which releases bound water molecules or other small molecules, and the destruction of the triple helix structure and peptide chain backbone of collagen.[33] The temperature at the maximum mass loss rate was calculated from DTG curves, which corresponded to the decomposition temperature (T_d) of the material.[32] The T_d of OL-pA gradually increased with the increase of its dosage from 4% to 12%. When the amount of OL was 12%, the T_d was 335 °C, which was 23 °C higher than that before the reaction and continuing to increase the amount had little effect on the T_d. In addition, the T_d of LH-pA was smaller than that of OL-pA at the same amount of crosslinker, which was due to the stronger covalent bond between OL and pADM makes the molecular structure of OL-pA more stable and requires more energy for structural decomposition, that was consistent with the results of DSC. The above results showed that there was a strong interaction between OL and collagen. The molecular structure of OL-pA is more stable and the thermal stability is stronger after OL crosslinking.

Hydrophobicity–hydrophilicity analysis

The increased hydrophilicity of the artificial heart valve facilitates the rapid rehydration of the material after implantation into the human body to promote cell adhesion and proliferation on the surface of the material. Fig. 6 shows the moisture rate, the water absorption rate and the capillary water absorption rate of pADM, LH-pA and OL-pA. The results showed that the moisture rate and the water absorption rate of OL-pA increased with the increase of OL dosage, which was significantly higher than that of pADM ($P < 0.05$). This is due to the good hydrophilicity of OL, which contains a large number of polar groups such as carboxyl, sulfonic acid and hydroxyl groups. After crosslinking with pADM, the hydrophobic amino groups between collagen fibers are consumed and more oxygen-containing groups are introduced, it increases the number of hydrophilic groups of the material and improves the surface wettability of the material. In summary, the results showed that the hydrophilicity of OL-pA material was improved, which was very useful for using it as a biomaterial for heart valves.

Enzymatic degradation resistance analysis

The degradation of artificial heart valves has a direct impact on their durability and long-term stability. The main component of pADM is type I collagen, so type I collagenase was chosen to characterize the degradation ability of crosslinked materials. As seen in Fig. 7, pADM, LH-pA, and OL-pA were all degraded to some extent in type I collagenase solution. Compared with the degradation rate of pADM at each time point, the degradation rate of LH-pA decreased slightly, while the degradation rate of OL-pA all decreased significantly ($P < 0.05$). This indicates that the strong covalent crosslinking between OL and pADM significantly improved the structural stability and degradation resistance of OL-pA, which was consistent with the improvement of thermal stability of OL-pA. Especially after 7 days of collagenase treatment, pADM was completely degraded, the degradation rate of LH-pA was 77%, while the degradation rates of 12% -OL-pA and 16% -OL-pA were less than 20%. The results strongly demonstrated that the use of OL crosslinking could greatly improve the biochemical stability of pADM, significantly enhance the enzymatic degradation resistance and reduce the degradation rate of OL-pA.

Cytocompatibility analysis

Excellent cell compatibility is essential for the clinical application of artificial heart valves. Cell adhesion and proliferation on

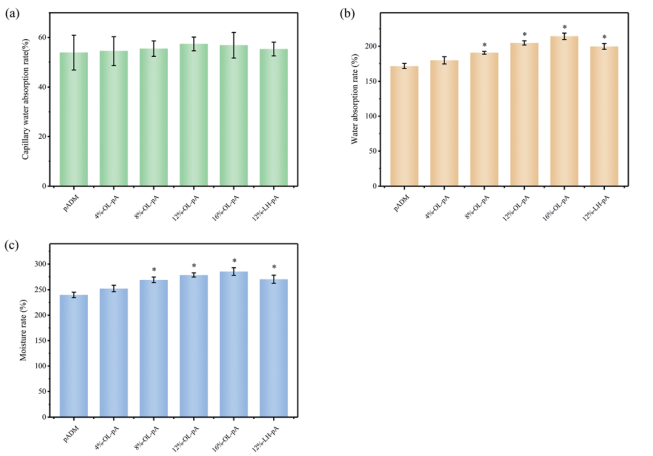

Fig. 6 (a) Capillary water absorption rate, (b) water absorption rate and (c) moisture rate of pADM, LH-pA and OL-pA crosslinked with different dosage of OL.

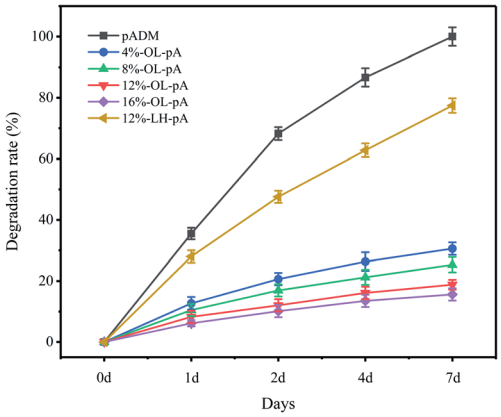

Fig. 7 Resistance to degradation of pADM, LH-pA and OL-pA crosslinked with different dosage of OL.

valve materials is the premise of tissue repair and regeneration. The cytocompatibility of the samples was evaluated by CCK-8 method. Fig. 8 shows the relative proliferation rate (RGR) of L929 fibroblasts in each group of extracts with polystyrene pores as a control. pADM is the aggregation of collagen fibers, it can act as an attachment and scaffold for cell growth and promote cell adhesion, proliferation and differentiation on its surface.[34,35] The results showed that both LH-pA and OL-pA could promote the adhesion, growth and proliferation of cells because heparin molecules grafted on the surface of pADM could promote the adsorption of fibronectin, thereby promoting the adhesion and proliferation of cells.[36] Among them, 12%-OL-pA showed the best cytocompatibility in all samples. When the OL dosage was less than 12%, the RGR of OL-pA increased with increasing OL dosage and was significantly higher than that of pADM ($P < 0.05$). This indicated that at a certain concentration, low dose OL crosslinking could significantly promote cell proliferation, and the crosslinking materials had almost no cytotoxicity. However, when the dosage of OL was greater than 12%, the RGR of the high dose OL-pA

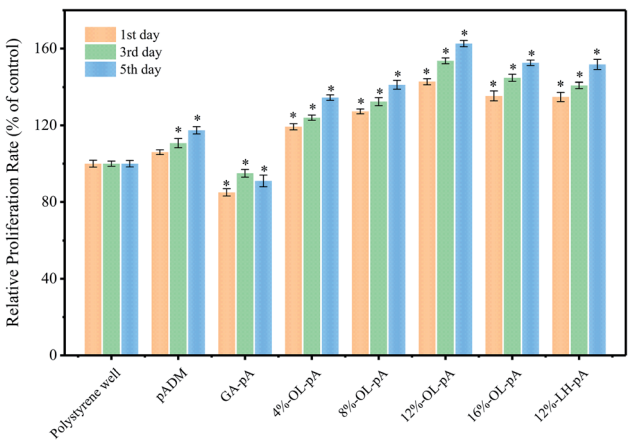

Fig. 8 Proliferation of L929 fibroblasts cultured in the extraction liquid of pADM, GA-pA, LH-pA and OL-pA crosslinked with different dosage of OL.

was reduced, it may be due to the excessive aldehyde group reaction being incomplete and remains on the surface of pADM, which reacts with proteins and polysaccharides in fibroblasts, resulting in the decrease of RGR.

GA and OL both were crosslinked with collagen through the aldehyde group, but the RGR of GA-pA was the smallest in all samples. For GA is an artificially synthesized exogenous cross-linking agent, and when it is used for pADM cross-linking, some naked aldehyde groups that are not involved in the reaction would destroy the morphological function and metabolism of cells on the surface of pADM, and then lead to apoptosis. While LMWH is a natural polysaccharide extracted from liver and small intestine mucosa. The main structure of OL after oxidation by sodium periodate is still the natural molecular chain of heparin, and its biocompatible conformation largely compensates for the negative effect of the aldehyde group on the cell proliferation situation, which is one of the advantages of using OL for crosslinking pADM. In conclusion, the results showed that the cytocompatibility of OL-pA crosslinked with different dosage of OL were all grade 0, with almost no cytotoxicity, it could induce cell adhesion, proliferation and growth, meeting the requirements for the use of human implant materials.

Blood compatibility analysis

Coagulation is mainly caused by the interaction of activated platelets and coagulation factors with pADM. Platelet adhesion test is considered a direct method to characterize the anticoagulant properties of materials. Fig. 9a shows that the surfaces of pADM and GA-pA appeared a large amount of platelet adhesion and aggregation, some platelets were in a heavily activated state with pseudopods protruding. In contrast, the number of platelets adhered to the OL-pA surface was significantly reduced, and most of the platelets were round and not activated. When the dosage of OL was 12%, the number of platelets adhering to the surface of OL-pA was the lowest and significantly less than that of LH-pA at the same dosage ($P < 0.05$). This is because type I collagen in pADM could specifically recognize and bind to an integrin receptor on platelets through integrin $\alpha 2\beta 1$, resulting in accelerated aggregation of platelets in the blood on the collagen surface.[37] Collagen can also activate platelets to further release coagulation factors and accelerate the endogenous coagulation mechanism of the body. These two effects reinforce each other and lead to the aggregation of a large number of activated platelets on the surface of pADM. These platelet aggregates will form thrombosis and are extremely easy to cause postoperative complications such as thrombocytopenia and bleeding when directly used in heart valve materials, seriously affecting the patient's treatment outcome and surgical safety. Heparin is an anionic polysaccharide with a negative charge.[38] Its main constituent groups are carboxylic acid groups, sulfonic acid groups and other anionic groups, so it can produce electrostatic repulsion with the negative charge on the platelet surface and reduce the massive adsorption of plasma proteins and blood cells on the surface of the material, and its anti-platelet adhesion properties are remarkable.[39,40] Therefore, the cross-linking of LMWH and

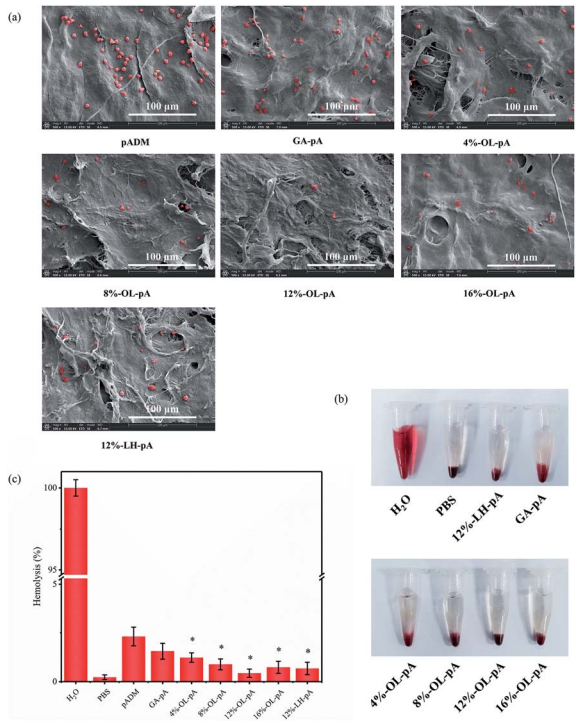

Fig. 9 (a) SEM photographs of platelet adhesion, (b) hemolysis phenomenon and (c) hemolysis rate of pADM, GA-pA, LH-pA and OL-pA crosslinked with different dosage of OL.

pADM can reduce the number of platelets adhered to pADM, but LMWH and pADM are combined by physical adsorption, and the combination of pADM and LMWH is weak, which can only improve the anti-platelet adhesion performance of pADM in a short time. As the interaction time between the material and blood increases, most of the unfixed heparin will be released and lost from the surface of the material with the flow of blood, so the anti-platelet adhesion and anti-coagulation properties of LH-pA will be greatly reduced when it is exposed to the blood environment for a long time. In contrast, the stronger cross-linking of the aldehyde group of OL with the amino group of pADM can immobilize the heparin molecule on the surface of the material through covalent bonding, avoiding the destruction of the anticoagulant active center of the heparin molecule. That can significantly improve and maintain the anti-platelet adhesion and anticoagulant effect of OL-pA in the blood environment in the long term. In conclusion, the improvement of anti-platelet adhesion properties of OL-pA is the result of the synergistic balance between collagen in pADM and heparin molecules, that is, heparin is the dominant anti-platelet adhesion molecule. Compared with pADM and GA-pA, the surface of OL-pA is not easy to be adhered, aggregated and activated by platelets. The anti-platelet adhesion performance is very obvious, and its blood compatibility and biocompatibility have been significantly improved.

Hemolysis is a phenomenon that red blood cells are destroyed and hemoglobin is released, and the hemolysis rate is directly related to the safety of prosthetic heart valve implantation. It can be visualized from Fig. 9b that no significant hemolysis was observed in OL-pA, LH-pA and GA-pA. The hemolysis rate in Fig. 10c showed that all groups of OL-pA were significantly smaller than those of pADM ($P < 0.05$). 12%-OL-pA had the lowest hemolysis rate of 0.436%, and the hemolysis rates of the remaining groups of OL-pA were less than 1%, which was much smaller than the upper limit of 5% specified in the international standard. This indicates that the OL-pA material has a very low degree of destruction of red blood cells, and its implantation into the body will not cause hemolysis, which meets the safety standards for blood contact materials and has good blood safety.

In vitro anticoagulant activity analysis

Anticoagulant performance is an important indicator for the evaluation of biomaterials contacted with blood, it is also crucial for the implantation of human heart valves. Under *in vitro* static conditions, the anticoagulant function is mainly reflected in the extension of coagulation time. APTT, PT and TT are often used to characterize the anticoagulant activity of the sample, and the three indicators reflect the coagulation of the endogenous coagulation system, the exogenous coagulation system and the conversion of plasma fibrinogen to fibrin. As shown in Fig. 10, the APTT, PT and TT of pADM was short, and the APTT, PT and TT of GA-pA was slightly prolonged, but it was not obvious. Compared with pADM and GA-pA, APTT, PT and TT of OL-pA were significantly prolonged ($P < 0.05$). Compared with LH-pA, PT and TT of OL-pA had no significant difference, and the APTT although decreased were still significantly higher than those in pADM and GA-pA. It has been known that the main component of pADM is collagen, it will cause the adhesion and aggregation of platelets when it is exposed to the blood, as well as activate the coagulation system to release coagulation factors and thrombin, inducing pro-fibrin aggregation to form stable fibrin multimers and produces clots.[41] Therefore, the anticoagulant activity of pADM is very poor, it is easy to activate platelets and form thrombus when it is in contact with blood after implantation, leading to vascular blockage or hemorrhage,

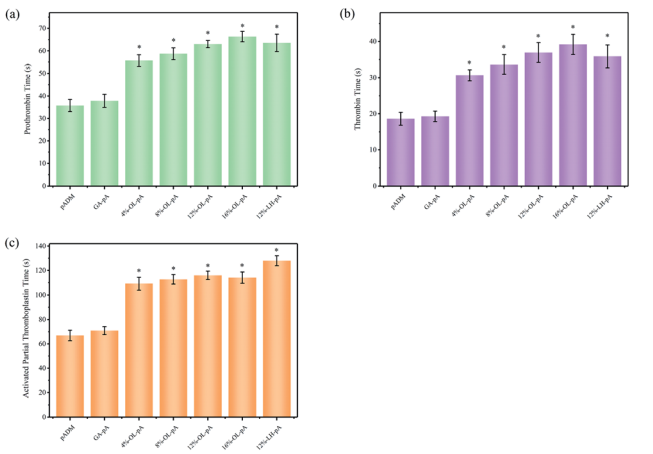

Fig. 10 (a) Prothrombin time, (b) thrombin time and (c) activated partial thromboplastin time of pADM, GA-pA, LH-pA and OL-pA crosslinked with different dosage of OL.

which can seriously threaten the life safety of patients during operation. The anticoagulant property of GA-pA was slightly enhanced because the introduction of GA crosslinking agent would reduce the hydrophilic group of the collagen molecular chain, resulting in a decrease in the hydrophilicity of pADM and thus a certain anticoagulant effect. However, compared with LH-pA and OL-pA, the improvement of the anticoagulant effect of GA-pA was almost negligible.

As the most widely used anticoagulant drug in heart valve surgery, the anticoagulant activity of LMWH is related to the pentose structure, sulfonic acid, carboxylic acid and other groups on its molecular chain. The pentose structural domain in its molecule can effectively activate antithrombin (ATIII), change the conformation of the arginine active center of ATIII, inhibit the activity of coagulation factors IIa and Xa, delay the formation of the fibrin network, and strengthen the anticoagulant effect of the endogenous coagulation system, which is mainly reflected in the prolongation of APTT. In addition, LMWH can enhance the anticoagulant effect by activating HCII and inactivating thrombin, which is mainly reflected in the prolongation of PT and TT. But the anticoagulant activity of heparin is too significant, which is likely to lead to blood dysfunction, thrombocytopenia and massive bleeding in patients with excessive anticoagulation due to anticoagulation overload even directly threaten life safety of patients when it is directly used for artificial heart valve implantation.[42] According to FTIR and UV results, the molecular structure of OL was similar to that of LMWH, and still contained a pentose structure of anticoagulant activity. The breakage of the C–C bond of the main chain during the oxidation of sodium periodate may had some effect on the structure of pentose in the heparin molecule. Thus, the APTT of OL-pA is longer than that of pADM, but shorter than that of LH-pA, the APTT among the OL-pA with different dosage of OL did not differ much. The PT and TT were mainly related to the dosage, so the PT and TT of 12% -LH-pA and 12% -OL-pA did not differ significantly, and the PT and TT of OL-pA enhanced with the increase of OL dosage.

In summary, the improved anticoagulant properties of OL-pA are the result of the synergistic balance between the collagen in pADM and the heparin molecule in terms of coagulation properties, *i.e.*, the heparin molecule dominates the anticoagulant properties. Compared with pADM, the anticoagulant properties of OL-pA were significantly improved, and the anticoagulant activity of the heparin molecule was well maintained, and the anticoagulant effect of OL-pA was milder. It can reduce the incidence of complications such as coagulation, thrombocytopenia and bleeding when it is used as *in vivo* implant materials in direct contact with human blood. This makes OL have a broader clinical application in the field of anticoagulant performance modification of artificial heart valves.

Conclusions

In summary, the dialdehyde oxidize low molecular weight heparin (OL) with anticoagulant activity was prepared using sodium periodate in this study, and the feasibility of OL as a novel cross-linking agent for modifying the anticoagulant and anti-platelet properties of pADM was further demonstrated. The OL obtained after oxidation with sodium periodate still retains the natural molecular structure and anticoagulant active groups of heparin, and its molecule contains the crosslinking active aldehyde groups, which can combine with the amino groups in collagen molecules to generate a large number of stable Schiff bases. This covalent crosslinking effect is stronger, and it is conducive to maintaining the stability of cardiac valve materials in long-term use. Compared with pADM, GA-pA and LH-pA, OL crosslinking can improve the thermal stability and biological stability of pADM, making it more stable thermal degradation resistance and enzyme degradation resistance. The OL-pA treated with the appropriate amount of OL can significantly promote cell adhesion, proliferation and growth, and their cytocompatibility were all grade 0, almost no cytotoxicity, which meet the requirements of human implant material. The surface of OL-pA is not easy to be adhered, aggregated and activated by platelets. The anti-platelet adhesion performance is significantly improved, and the hemolysis rate is less than 1%. Implanting this type of material into the human body will hardly destroy red blood cells and hardly cause hemolysis, which meets the safety standards of blood contact materials. Most importantly, the anticoagulant effect of OL-pA was significantly improved, and the anticoagulant activity of heparin molecules was well maintained. Moreover, the anticoagulant effect of OL-pA was milder, which to some extent weakens the side effects such as bleeding that may occur when OL-pA is applied to implant materials *in vivo*, that makes OL have a broader clinical application prospect in the field of anticoagulant performance modification of artificial heart valves.

In summary, OL is a very effective anticoagulant crosslinking agent, it can impart excellent anticoagulant properties and blood compatibility to collagen-based materials. It is expected to be applied to the modified preparation and clinical application of anticoagulant stent materials such as heart valves and artificial blood vessels.

Conflicts of interest

The authors declare that they have no known competing financial interests or personal relationships that could have appeared to influence the work reported in this paper.

Acknowledgements

This research was supported by the Opening Project of Key Laboratory of Leather Chemistry and Engineering, (Sichuan University), Ministry of Education (SCU2021D005), the National Natural Science Foundation of China Youth Science Foundation Project (32101081), and the Fundamental Research Funds for the Central Universities (20826041E4156).

References

1 M. W. Sherwood and T. L. Kiefer, *Curr. Cardiol. Rep.*, 2017, **19**, 130.

2 F. Peeters, S. J. R. Meex, M. R. Dweck, E. Aikawa, H. Crijns and L. J. Schurgers, *Eur. Heart J.*, 2018, **39**, 2618–2624.
3 C. M. Otto, R. A. Nishimura, R. O. Bonow, B. A. Carabello, J. P. Erwin and F. Gentile, *Circulation*, 2021, **143**, e35–71.
4 E. A. RodríguezCaulo, O. R. BlancoHerrera and E. Berastegui, *J. Thorac. Cardiovasc. Surg.*, 2021, **01**, 118.
5 M. H. Veltrop and H. Beekhuizen, *J. Infect. Dis.*, 2002, **186**, 1145–1154.
6 L. Liesenborghs, S. Meyers and T. Vanassche, *J. Thromb. Haemostasis*, 2020, **18**, 995–1008.
7 C. E. Garcia, H. N. Fernandez and B. Almirante, *Circulation*, 2013, **127**, 2272–2284.
8 C. M. Otto, R. A. Nishimura, R. O. Bonow, B. A. Carabello, J. P. Erwin, F. Gentile, H. Jneid, E. V. Krieger, M. Mack and C. M. Leod, *J. Thorac. Cardiovasc. Surg.*, 2021, **162**, e183–e353.
9 A. Vahanian, F. Beyersdorf, F. Praz, M. Milojevic, S. Baldus and J. Bauersachs, *Eur. J. Cardio. Thorac. Surg.*, 2021, **60**, 727–800.
10 Y. Hu, W. H. Dan, S. J. Xiong, Y. Kang, A. Dhinakar, J. Wu and Z. Gu, *Acta Biomater.*, 2017, **47**, 135.
11 X. H. Liu, F. Li and Q. Huang, *J. Am. Leather Chem. Assoc.*, 2016, **111**, 447.
12 L. Liesenborghs, P. Verhamme and T. Vanassche, *J. Thromb. Haemostasis*, 2018, **16**, 441–454.
13 Y. Hu, W. H. Dan and S. J. Xiong, *Acta Biomater.*, 2017, **47**, 135.
14 S. Zhu, Z. Gu, Y. Hu, W. H. Dan and S. J. Xiong, *Appl. Polym. Sci.*, 2016, **133**, 43550.
15 T. Liu, L. Shi, Z. Gu, W. H. Dan and N. H. Dan, *Int. J. Biol. Macromol.*, 2017, **101**, 889.
16 C. Hao, M. J. Sun, H. M. Wang, L. J. Zhang and W. Wang, *Prog. Mol. Biol. Transl. Sci.*, 2019, **163**, 21–39.
17 P. Sarantis, A. Bokas, A. Papadimitropoulou, E. Koustas, S. Theocharis and P. Papakotoulas, *Int. J. Mol. Sci.*, 2021, **22**, 7053.
18 A. Bokas, P. Papakotoulas, P. Sarantis, A. Papadimitropoulou, A. G. Papavassiliou and M. V. Karamouzis, *Cancers*, 2020, **12**, 432.
19 U. Ejaz, F. Akhtar, J. Xue, X. Wan, T. Zhang and S. He, *Eur. J. Pharmacol.*, 2020, **13**, 1095.
20 X. H. Liu, Z. Yan, X. Wang, X. Luo, T. Qiang and W. Dan, *ACS Sustainable Chem. Eng.*, 2018, **6**, 17142.
21 H. Mozafari, M. Hojjatoleslamy and M. Mohammadizadeh, *Int. J. Biol. Macromol.*, 2020, **167**, 413.
22 T. Liu, L. Shi, Z. Gu, W. H. Dan and N. H. Dan, *Int. J. Biol. Macromol.*, 2017, **101**, 889.
23 J. B. Xie, J. Wan and X. M. Tang, *Transl. Androl. Urol.*, 2021, **10**, 3656–3668.
24 Z. Najarzadeh, M. Zaman and V. Sereikaite, *J. Biol. Chem.*, 2021, **297**, 100953.
25 S. Fazil, H. Shah and M. Noreen, *J. King Saud Univ. Sci.*, 2021, **33**(6), 612.
26 X. H. Liu, N. H. Dan, W. H. Dan and J. X. Gong, *Int. J. Biol. Macromol.*, 2016, **82**, 989.
27 S. W. Xiao, W. H. Dan and N. H. Dan, *RSC Adv.*, 2015, **5**, 88324.
28 X. H. Liu, W. H. Dan, H. Ju, N. H. Dan and J. X. Gong, *RSC Adv.*, 2015, **5**, 52079.
29 X. H. Liu, N. H. Dan and W. H. Dan, *Mater. Sci. Eng., C*, 2017, **70**, 689.
30 Y. N. Chen, N. H. Dan and S. J. Xiao, *Leather Technol. Chem.*, 2018, **102**, 12.
31 P. B. Jr and N. S. Levine, *Arch. Surg.*, 1984, **119**, 312.
32 X. H. Liu, N. H. Dan, W. H. Dan and J. X. Gong, *Int. J. Biol. Macromol.*, 2016, **82**, 989.
33 X. H. Liu, Z. Yan, X. Wang, X. Luo, T. Qiang and W. H. Dan, *ACS Sustainable Chem. Eng.*, 2018, **6**, 17142.
34 X. H. Liu, Z. Yan, X. Wang, X. Luo, T. Qiang and W. H. Dan, *ACS Sustainable Chem. Eng.*, 2018, **6**, 17142–17151.
35 Y. Hu, Y. Zhu and X. Zhou, *J. Mater. Chem. B*, 2016, **4**, 1235.
36 Y. Ding, M. Yang, Z. Yang, R. Luo, X. Lu, N. Huang, P. Huang and Y. Leng, *Acta Biomater.*, 2015, **15**, 150–163.
37 E. Anitua, M. Zalduendo and M. Troya, *Ann. Anat.*, 2021, **236**, 151853.
38 Y. Ji, Y. Wang and W. Zeng, *Carbohydr. Polym.*, 2020, **249**, 116824.
39 X. L. Qiu, Z. R. Fan, Y. Y. Liu, D. F. Wang, S. X. Wang and C. X. Li, *Int. J. Mol. Sci.*, 2021, **22**, 4077.
40 G. H. Fang and B. Tang, *Asian J. Pharm. Sci.*, 2020, **15**, 449–460.
41 X. H. Liu, H. Hou and M. D. Luo, *Biomacromolecules*, 2021, **124**, 149–155.
42 C. Hao, M. J. Sun and H. M. Wang, *Prog. Mol. Biol. Transl. Sci.*, 2019, **163**, 21–39.